A&A 595, A34 (2016)
DOI: 10.1051/0004-6361/201629045

Astronomy & Astrophysics

The upGREAT 1.9 THz multi-pixel high resolution spectrometer for the SOFIA Observatory⋆

C. Risacher[1], R. Güsten[1], J. Stutzki[2], H.-W. Hübers[3] A. Bell[1], C. Buchbender[2], D. Büchel[2], T. Csengeri[1], U. U. Graf[2], S. Heyminck[1], R. D. Higgins[2], C. E. Honingh[2], K. Jacobs[2], B. Klein[1,5], Y. Okada[2], A. Parikka[2], P. Pütz[2], N. Reyes[1,4], O. Ricken[1], D. Riquelme[1], R. Simon[2], and H. Wiesemeyer[1]

[1] Max-Planck-Institut für Radioastronomie, Auf dem Hügel 69, 53121 Bonn, Germany
e-mail: crisache@mpifr.de
[2] I. Physikalisches Institut der Universität zu Köln, Zülpicher Strasse 77, 50937 Köln, Germany
[3] Institute of Planetary Research, German Aerospace Center (DLR), Rutherfordstr. 2, 12489 Berlin, Germany
[4] Departamento de Ingeniería Eléctrica, Universidad de Chile, 1085 Santiago, Chile
[5] University of Applied Sciences Bonn-Rhein-Sieg, 53757 Sankt Augustin, Germany

Received 2 June 2016 / Accepted 18 July 2016

ABSTRACT

We present a new multi-pixel high resolution ($R \gtrsim 10^7$) spectrometer for the Stratospheric Observatory for Far-Infrared Astronomy (SOFIA). The receiver uses 2 × 7-pixel subarrays in orthogonal polarization, each in an hexagonal array around a central pixel. We present the first results for this new instrument after commissioning campaigns in May and December 2015 and after science observations performed in May 2016. The receiver is designed to ultimately cover the full 1.8−2.5 THz frequency range but in its first implementation, the observing range was limited to observations of the [CII] line at 1.9 THz in 2015 and extended to 1.83−2.07 THz in 2016. The instrument sensitivities are state-of-the-art and the first scientific observations performed shortly after the commissioning confirm that the time efficiency for large scale imaging is improved by more than an order of magnitude as compared to single pixel receivers. An example of large scale mapping around the Horsehead Nebula is presented here illustrating this improvement. The array has been added to SOFIA's instrument suite already for ongoing observing cycle 4.

Key words. instrumentation: spectrographs – techniques: spectroscopic

1. Introduction

Far-infrared astronomy has seen an enormous breakthrough with the observations of the *Herschel* satellite, which was active between 2009−2013 (Pilbratt et al. 2010). *Herschel* revolutionized our understanding of many astrophysical processes (star formation, planetary science, etc.) and so far resulted in more than 1600 refereed publications as of early 2016.

Since 2011, observations at infrared wavelengths 0.3−1600 μm can be performed with the NASA/DLR airborne observatory SOFIA[1], carrying a 2.5 m telescope onboard a Boeing 747−SP aircraft (Young et al. 2012). It currently operates a suite of six instruments available to the interested communities covering wavelength ranges not observable from ground-based facilities: EXES (Richter et al. 2010), FIFI-LS (Klein et al. 2010), FLITECAM (Smith & McLean 2008), HIPO (Dunham et al. 2008), FORCAST (Adams et al. 2010) and GREAT (Heyminck et al. 2012). The HAWC+ instrument (Vaillancourt et al. 2007) is currently in its commissioning phase in 2016. Among those instruments, the only one able to perform high resolution spectroscopy (above 10^7 resolving power) is the GREAT instrument[2]. The other instruments employ continuum detectors and only offer low- to mid-resolution capabilities (except EXES which can go up to 10^5 resolving power). High resolution is needed in order to resolve the spectral lines profiles, which in turn allows studying the gas kinematics in great detail.

Until now, only single pixel receivers had been achieved in a handful of observatories for frequencies above 1 THz. The Max-Planck-Institut für Radioastronomie in Bonn, together with the I. Physikalisches Institut der Universität zu Köln and the Institute of Planetary Research, (DLR, Berlin), are building a new generation of multi-pixel high resolution spectrometers for the SOFIA NASA/DLR project, the upGREAT THz arrays. They consist of dual-color array receivers (for different frequency bands), which will ultimately operate in parallel. The Low Frequency Array (LFA) is designed to cover the 1.8−2.5 THz range using 2 × 7-pixel waveguide-based HEB mixer arrays in dual polarization configuration and double sideband mode. The High Frequency Array (HFA) will perform observations of the [OI] line at 4.745 THz using a 7-pixel waveguide-based HEB mixer array, in double sideband mode. We present here the results from the upGREAT/LFA commissioning, which is the first multipixel array

⋆ The datacube of the Horsehead observations is only available at the CDS via anonymous ftp to cdsarc.u-strasbg.fr (130.79.128.5) or via http://cdsarc.u-strasbg.fr/viz-bin/qcat?J/A+A/595/A34

[1] SOFIA is a joint project of NASA and the German Aerospace Center (DLR). The aircraft is based at the NASA Armstrong Flight Research Center (AFRC) facility in Palmdale, California which also manages the program. NASA Ames Research Center at Moffett Field, CA, USA, manages the SOFIA science and mission operations in cooperation with the Universities Space Research Association (USRA) headquartered in Columbia, MD, USA, and the German SOFIA Institute (DSI) at the University of Stuttgart.

[2] GREAT is developed by the MPI für Radioastronomie and the KOSMA/Universität zu Köln, in cooperation with the MPI für Sonnensystemforschung and the DLR Institut für Planetenforschung.

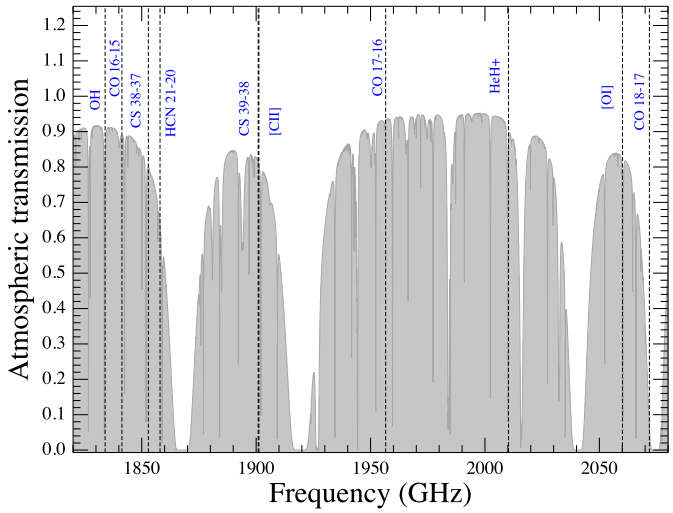

Fig. 1. upGREAT LFA receiver coverage for observing cycle 5 and atmospheric transmission for the SOFIA telescope when flying at an altitude of 40 000 feet with a PWV of 15 μm. Important spectral lines are indicated.

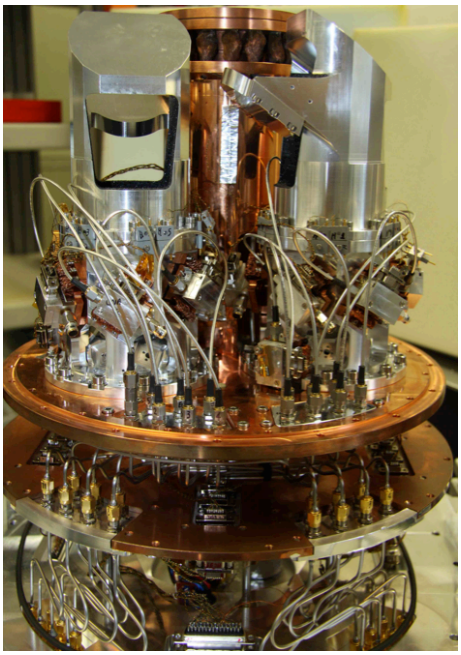

Fig. 2. View of the inside of the upGREAT-LFA cryostat showing the different cold stages, part of the optics, and electronic connections.

for high resolution spectroscopy successfully built and deployed on a telescope for this frequency range. This paper complements the technical description of the instrument (Risacher et al. 2016) with information about the actual on-sky performance and dedicated observing strategies relevant to interested users.

2. Instrument description

2.1. Frequency coverage and atmospheric transmission

The far-infrared regime (1−10 THz) is largely blocked by the Earth's atmosphere. Only very narrow windows with low transmission become accessible from dry high-altitude sites for frequencies above 1 THz. To overcome the atmospheric attenuation, airborne telescopes, high-altitude balloons and satellites are the only platforms that allow performing such observations. Figure 1 shows the typical atmospheric transmission when SOFIA is flying at 40 000 feet, with average atmospheric conditions (residual precipitable water vapor PWV of 15 μm). The upGREAT/LFA receiver array is designed to cover the 1.8−2.5 THz frequency range, whose most important lines are listed in Table 1. Among the main atomic and molecular tracers are [CII], [OI], HeH^+, OH and CO via its rotational transition ladder from $J = 16-15$ to $J = 22-21$. For the commissioning and first flights, the tuning range was limited to the [CII] line transition at 1900 GHz by the available local oscillator (LO) reference signal. The 1.83−2.07 THz range has been available since May 2016. We foresee that in the coming years with improved technology, the remaining of the tuning range will be covered.

Table 1. Main atomic and molecular transitions accessible to upGREAT/LFA.

Species	Rest freq.	Transition	Comment
OH	1.834 THz		
CO	1.841 THz	$J = 16-15$	
CII	1.9005 THz	$J = 3/2-1/2$	
CO	1.955 THz	$J = 17-16$	
HeH^+	2.01 THz		
OI	2.06 THz		
CO	2. 07THz	$J = 18-17$	close to atmospheric feature
CO	2.42 THz	$J = 20-21$	not tunable yet
OH	2.49 THz		not tunable yet
OH	2.51 THz		not tunable yet
CO	2.52 THz	$J = 21-20$	not tunable yet

2.2. Instrument hardware

The upGREAT receiver is described in detail in Risacher et al. (2016). For high resolution spectroscopy at frequencies above 1 THz, the technology of choice for the detectors is based on hot electron bolometers (HEB) superconducting mixers (Shurakov et al. 2016) and therefore, the instrument needs to be cooled to temperatures well below 6 K. Until now, such heterodyne receivers incorporated only up to a few mixers (e.g., Graf et al. 2015). Therefore, integrating 14 such mixers for the upGREAT/LFA receiver represents a considerable technological challenge and a major step forward. All first generation GREAT receivers operate single mixers for frequencies between 1.2 THz and 4.7 THz (Heyminck et al. 2012). The HEB mixers are developed and fabricated by the I. Physikalisches Institut der Universität zu Köln (Pütz et al. 2012, Büchel et al. 2015).

A view of the upGREAT/LFA cryostat is shown in Fig. 2, illustrating the dense packaging of the components. Figure 3 shows the whole instrument when installed on the SOFIA telescope. The LFA cryostat is cooled with a closed-cycle pulse tube refrigerator suitable for the superconducting detectors. Table 2 lists the main receiver characteristics. The receiver consists of two sub-arrays of 7 pixels each, having orthogonal polarizations, and placed in a hexagonal configuration around co-aligned central pixels.

The spectrometer backends are the last generation of fast Fourier transform spectrometers (FFTS; Klein et al. 2012) developed at the Max-Planck-Institut für Radioastronomie, Bonn. They achieve an instantaneous intermediate frequency (IF) bandwidth of 4 GHz per pixel, with a spectral resolution of 142 kHz, which translates to a total spectral bandwidth of about 630 km s^{-1} and a resolution of 0.022 km s^{-1} at the frequency of the [CII] line.

Table 2. upGREAT LFA receiver characteristics.

Parameter	Performance	Comment
RF bandwidth	1.81−2.54 THz	goal bandwidth
	1.83−2.07 THz	currently usable RF bandwidth
IF bandwidth	0.2−4 GHz	full usable IF range (3dB roll-off)
Receiver sensitivity	1800 K SSB	at 2 GHz IF (average over all pixels)
System noise temperature	2000 K SSB	for PWV < 15 μm
Number of pixels	7 per sub-array (14 total)	dual polarization
Backends	4 GHz instantaneous BW	FFTS technology
Array geometry	hexagonal arrays with central pixel	

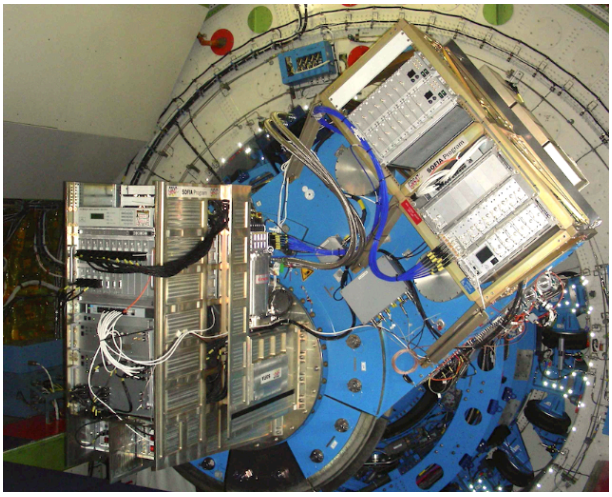

Fig. 3. upGREAT instrument mounted on the SOFIA telescope.

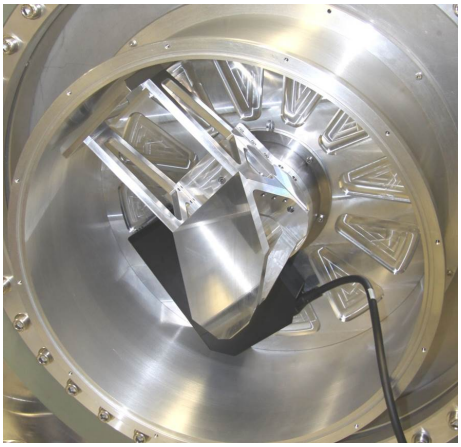

Fig. 4. Derotator consisting of three high quality optical flat mirrors, mounted on a rotation stage, can compensate for the sky rotation to keep the array pattern in the instrument internal focal plane constant.

2.3. Derotator

With the upGREAT arrays, a derotator (implemented as a so-called K-mirror) is needed to compensate for the sky rotation in the instrument focal plane, which is fixed to the telescope (see Fig. 4). The SOFIA telescope is a 3-axis telescope, but has a limited travel range of only about ±3° in all axes for its fine drive. The telescope tracks celestial objects fixed in an inertial reference frame, keeping the relative orientation between the sky and the instrument focal plane fixed. When it gets close to the fine drive limit, the telescope is rewound to move close to the opposite limit, thus rapidly rotating the sky/instrument mounting flange focal plane orientation. The derotator then is turned oppositely, under computer control, by the same amount to keep the sky orientation in the instrument internal focal plane constant. The pixel pattern can then be kept fixed on sky (in the equatorial or horizontal reference system) and/or rotated as desired. Areas on the sky can therefore be efficiently homogeneously sampled, and a variety of observing strategies is possible.

3. Commissioning flights

3.1. Commissioning plan

The LFA was fully commissioned during a total of 5 flights, in May and December 2015. An example of one of the flight plans is shown in Fig. 5. For the upGREAT commissioning flights, the SOFIA airplane took off and landed in Palmdale, CA. The duration of the flights is typically about 10 h, of which 8.5 h are science observations.

During the first flights in May, the instrument could only operate one of the two 7 pixel sub-arrays at a time. For the December flights, this limitation was resolved and the 2×7 pixels were employed simultaneously. The activities performed during the commissioning were aimed at verifying:

(a) basic functionalities of the new hardware/software (incl. the K-mirror derotator);
(b) the array performance on sky, assessed measuring the sensitivities and stability of the instrument;
(c) determining the instrument focal plane geometry (boresight and pixels position on the sky);
(d) assessing the telescope optimal focus position;
(e) measuring the beam efficiencies on strong compact continuum objects;
(f) testing and evaluating various observing modes.

3.2. Observing modes

Observing with upGREAT on SOFIA is done with the kosma-control-software package, developed and used for several single-dish telescopes and instruments; it is also used by the FIFI-LS instrument on SOFIA. All observing modes that have been used for single pixel observations (Heyminck et al. 2012) were adapted for the upGREAT observations. In addition, we introduced two new observing modes specific for a hexagonal array. All observing modes work both for total power and chopped observations, the latter are performed by moving the telescope subreflector.

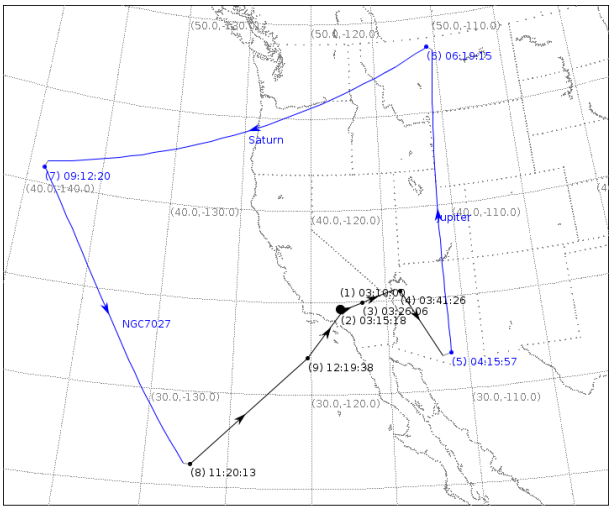

Fig. 5. Example of one of the LFA commissioning flights, performed on May 12th 2015. Indicated are the various targets observed during each of the flight legs, with Jupiter, Saturn and NGC7027 used for the commissioning.

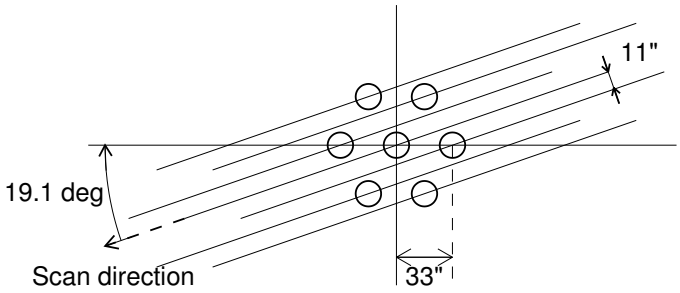

Fig. 6. Sketch of the array-OTF mapping mode. Circles indicate the half power beam-width (HPBW) in the hexagonal array pattern. The pixel spacing is 33″.

The first new observing mode is the array-optimized On-the-Fly (OTF) mapping mode (array-OTF mode). As shown in Fig. 6, scanning at 19.1 degrees against the axis of the hexagonal array makes an equally-spaced OTF scan with 7 pixels. To achieve a fully-sampled map, the array is scanned twice with a shift of 5.5″ perpendicular to the scan direction. In order to reduce unwanted systematic effects due to different sensitivities between pixels, two approaches to achieve redundant coverage are recommended. The first one consists in performing two orthogonal scans. The other one consists in rotating the array by 60 degrees or integer multiples thereof. In this case, the central pixel scans the same line on the sky. In science observations, this array-OTF mode is optimal for large-area mapping.

A dedicated observing mode has been developed for the pointing measurements (array-pointing mode) in order to determine the position of each pixel in the instrument internal focal plane and the rotator axis position in the instrument mounting flange focal plane (see Sect. 3.4). To determine those parameters, at least two scans with different scanning directions should go through each pixel for one beam rotator angle, and this set of observations should be repeated for at least three different rotator angles. This array-pointing mode consists of a set of scans, each of which is defined by two pixels that should hit the source (see example in Fig. 7).

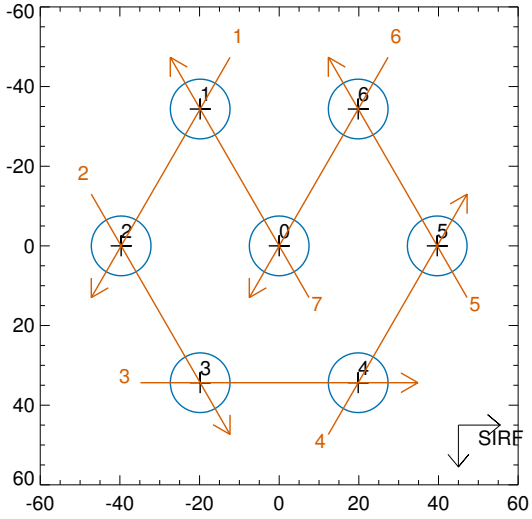

Fig. 7. Example of the pattern of the scans in the array-pointing mode. The unit of the x- and y- axes is in arcsec, and the direction of the axis follows the science instrument reference frame (SIRF), which is the coordinate system that we use for the pointing measurements. The black crosses with blue circles indicate the pixels with their HPBW of 15″, and the red arrows indicate the scan direction.

3.3. Instrument performance

3.3.1. Instrument sensitivities

The receiver sensitivities were verified during the flights with the regular calibration sequences, typically performed every 5 min. The instrument looks sequentially at a cold load and a hot load absorber. The cold load absorber is at a temperature of about 70 K, and is located in a small closed-cycle cryostat which is cooled with a Stirling cooler. The transmission of its high density polyethylene (HDPE) window was carefully characterized across the RF frequency range (transmission at 1.9 THz is about 84%). The hot load temperature is at about 293 K. An example of the instrument receiver noise temperatures at the [CII] frequency is shown in Fig. 8. Typically, the receiver noise temperatures are about 600 K−1000 K double-sideband (DSB) at the lower IF range and increasing to 1200 K−1800 K DSB at the high end of the IF bandwidth (4 GHz). During the flights, the typical precipitable water vapor was in the range 10−15 μm, which then results in a system temperature about 10−20% higher than the receiver temperatures shown, typically below 2000 K single-sideband (SSB) at the IF of the line of interest. Depending on the available LO power, large parts of the 1.83−2.07 THz range have comparable receiver performance. For some tunings, specially close to the edges, only one of the polarizations receives sufficient LO power.

3.3.2. Spectral purity

With the current local oscillator chains, there are some very narrow spurs in the IF passband located typically between 0.8 and 1.3 GHz and between 3.0−3.8 GHz. The spurs are narrower than the FFTS channel width. Those single channels can be removed easily during post-processing of the data. The positions of these interferences are not frequency dependent and they probably originate from electronic pickup noise in the multipliers bias lines.

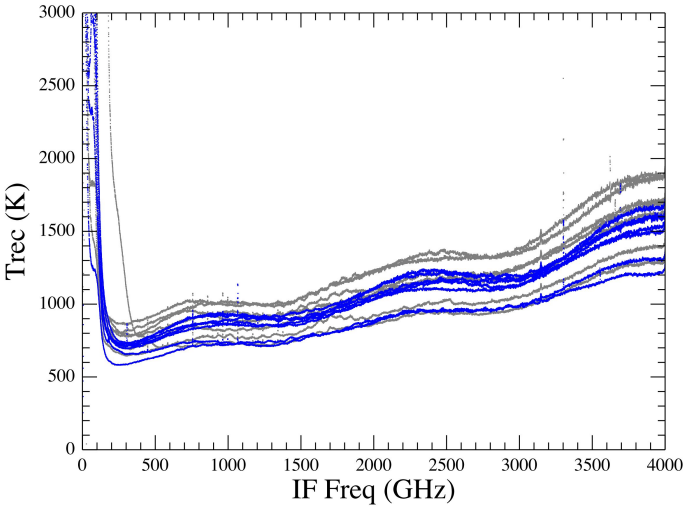

Fig. 8. Receiver performance showing the noise temperature for all 14 pixels. The typical receiver noise temperatures are about 600 K−1000 K DSB at the lower IF range and increase to 1200 K−1800 K DSB at the higher end of the IF bandwidth (4 GHz). The seven dark blue curves are for one of the sub-arrays (*H*-polarization) and the seven light gray curves show the other one (*V*-polarization).

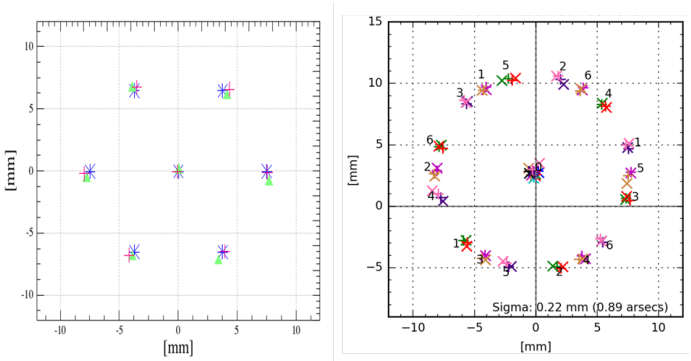

Fig. 9. Derived focal plane pixel positions from laboratory measurements for both LFA sub-arrays (*left plot*) shown with green triangles and red crosses, compared to the nominal designed positions plotted as blue crosses. The *right plot* shows the on-sky derivation of the pixel positions, performed for different derotator angles. The subarray positions are plotted using a same color, for example red and green are the *H* and *V* polarizations subarrays at a given derotator angle, then the other colors are taken for different angles. The (0, 0) for the plot refers to the SOFIA optical axis, which is different to the mechanical derotator axis. The rms deviations of the individual pixel positions of ∼0.22 mm around the nominal positions in an ideal hexagonal pattern, corresponds to 0.89″on the sky.

3.3.3. Baseline quality

Baseline qualities of double beam chopped observations (the chop frequency is 2.5 Hz) are very good, and generally require removal of zero or first order polynomials only. In case of background continuum, the quality is limited by the precision of removal of residual atmospheric features. The spectroscopic Allan variance time of the receiver channels is typically above 40 s, hence for long integrations per phase (i.e., position switched or long on-the-fly slews), some residual standing waves might be expected. The problem is exacerbated in observations asking for large offsets (at different airmass). Compared to the *Herschel*/HIFI bands 6 and 7 which used HEB mixers and whose baselines suffered from strong standing waves , there is a tremendous improvement in baseline quality with the upGREAT/LFA.

3.4. Boresight determination

The boresight determination is possible without a-priori knowledge of the exact array geometry. However, the relative positions of the pixels in the focal plane can be determined in the laboratory with a good accuracy (Graf 2016). This gives an estimate of the pixel positions on-sky, which will be corrected with pointing observations. The left plot of Fig. 9 shows the derived pixel positions in the focal plane when measured in the laboratory prior to the installation on SOFIA in May 2016.

The observations were done with the array pointing mode described in Sect. 3.3 (see Fig. 7). For these measurements, a bright compact source like a planet, is needed. In May 2015, Jupiter and Saturn were used, and in December 2015, as a planet was not available at the beginning of the observations, a strong barely resolved spectral line source was used (the young planetary nebula NGC 7027). For this, in addition to a cross scan pattern, a full map that includes the source in all pixels was used. This was the first time that a full map in the [CII] line was used to determine the array geometry. The measurements were verified with observations of Jupiter, available later in the flight series and subsequently used for the determination of the beam efficiencies. In May 2016, Jupiter was used for the boresight determination.

We parametrize the focal plane array geometry by the center offset from the derotator axis, and the scale-size and tilt of the ideal hexagonal footprint of each subarray. In a first step we thus fit this set of parameters to the set of measured pixel positions in the instrument mounting flange focal plane for at least three derotator angles. In a second step, we fit the offsets of each pixel relative to its nominal position in the ideal hexagonal subarray footprint to the set of measured positions. The former ones (i.e., the nominal pixel positions) are used to position the array and derotator angle when setting up on-the-fly mapping observations; the latter ones are used to record the proper, unavoidably slightly imperfect, pixel positions for the given derotator angle at the time of the observations in the raw data header information.

Both the array-pointing mode and full map resulted in rms deviations of the individual pixel positions of ∼0.22 mm around the nominal positions in an ideal hexagonal pattern, corresponding to 0.89″on the sky (right plot of Fig. 9), confirming that the original laboratory measurements were very close to the true pixel positions. The array central pixels were co-aligned within 0.5″. The single pixel receiver L1 (1.25−1.5 THz) is used simultaneously with the upGREAT/LFA receiver and the relative alignment between the L1 and the central pixels of the upGREAT LFA arrays was verified to be within 4″. The central LFA pixels were used for the tracking reference, therefore 4″ offset for the L1 beam is tolerable.

3.5. Beam efficiencies

The coupling efficiencies are determined from planets observations. Only Jupiter and Saturn were available so far, in May and December 2015, and in May 2016. We present the May 2016 results, where all of the 14 pixels were successfully operational. Jupiter was relatively extended (i.e., 39.5″ × 37.0″ on May 2016 relative to the half power full width of the diffraction limited beam of upGREAT: 15″at 1900 GHz) but well suited to determine and characterize the optical parameters of upGREAT. The derived main beam efficiencies for the upGREAT array are

Table 3. upGREAT LFA beam efficiencies derived from Jupiter observations in May 2016 at 1900 GHz.

Pixel	$\eta_{\mathrm{MB\ (Jupiter)}}$	Pixel	$\eta_{\mathrm{MB\ (Jupiter)}}$
H0	0.67 ± 0.03	V0	0.64 ± 0.04
H1	0.63 ± 0.02	V1	0.64 ± 0.03
H2	0.57 ± 0.02	V2	0.61± 0.03
H3	0.66 ± 0.01	V3	0.65 ± 0.02
H4	0.65± 0.02	V4	0.59 ± 0.03
H5	0.65 ± 0.03	V5	0.66 ± 0.03
H6	0.63 ± 0.02	V6	0.63 ± 0.03
Average	0.64	Average	0.63

Notes. The spread between pixels is of about ±5%. For each pixel, a 1σ rms level is indicated taken from 9 individual pointing measurements.

Table 4. upGREAT LFA beam parameters at 1.9 THz

Parameter	Measured value
Half power beam width	15.1″± 0.1″
Pixel spacing	33″± 0.2″
Edge taper (dB)	13 ± 0.2
Beam efficiencies	0.64 ± 0.03
Forward efficiencies	0.97 ± 0.01

typically 0.64 ± 0.03 and the spread between the various pixels can be seen in Table 3, and is of the order of 5%. Furthermore, for each pixel, these source was covered many times during the pointing measurements (9 scans), which provides an estimate of the measurement repeatability. The 1σ rms value is typically within 3%.

As the planetary models are typically accurate within ±5%, the derivation of the main beam efficiencies is estimated to be accurate within ±8%. The beam efficiencies are typically derived at the beginning of every flight series and the corresponding values are provided to the projects principal investigators (PI) together with the calibrated data.

3.6. Calibration accuracy

The calibration is based on the existing GREAT single pixel receiver calibration. The T_A^* calibration scale of GREAT is based on frequent (typically every 5 min) measurements of our integrated hot- cold reference loads. Corrections for atmospheric absorption are done with the kalibrate-task as part of the kosma-control software package, which is described together with the detailed calibration scheme in Guan et al. (2012).

In essence, a least square fit to all observed, gain-calibrated sky-hot spectra (all positions and all frequencies) with the precipitable water vapor above the observatory as the fit parameter, is used together with an appropriate atmospheric model to determine the sky-transmission. The observed and fitted sky temperatures are delivered to the PI with the data package, so they can appreciate the quality of the fit.

The default implementation is to treat every upGREAT pixel as a separate signal and the derived opacities might converge to different values for each pixel. The alternative scheme, which is being currently assessed, consists of using the pixels of each sub-array together and derive from them a best fit opacity value, which is then used for all pixels for the calibration. Observing with a receiver array, and hence obtaining independent measurements by each array pixel for the same atmosphere, allows to disentangle effects that are due to stability issues of the individual array pixels and effects from the atmosphere, that are common to all pixels. A detailed investigation of optimized calibration schemes is underway.

By far the largest contribution to the calibration uncertainties stems from the atmospheric corrections. It is estimated to be accurate within ±15% when free of strong atmospheric features. The closer the observation is from a strong feature, the worse the accuracy. The factors contributing to the overall calibration budget are:

- atmospheric calibration: ±15%;
- hot and cold load blackbody temperatures: ±2%;
- sideband ratios: ±5%;
- standing waves, compression effects: ±5%;
- beam efficiencies: ±8%;
- forward efficiencies: ±2%;

Therefore the overall calibration error is estimated to be within ±20%. The telescope pointing and tracking accuracy of 1″ or better is close to perfect for our 15″ beam.

4. First science observations

In May and December 2015, a total of five commissioning flights and five science flights were successfully performed. A variety of projects could be observed during those flights. We present here a few snapshots that illustrate the large scale mapping capabilities of the array. These observations were targeting the [CII] line, which mainly traces the ionized and atomic gas and the UV illuminated edges (also called photo-dominated regions, PDRs) of dense molecular gas clouds. It is one of the main coolants of the warm gas and hence very important for the study of star-formation.

4.1. W3OH

The very first spectral footprint of 14 pixels of the LFA array was taken on the compact HII region W3(OH). This source is associated with one of the strongest bipolar outflows with a velocity range of about 50 km s^{-1}. The region hosts several sites of ongoing star formation. The most prominent ones are the ultra-compact HII region itself, which is ionized by a young O star, and a region showing hot molecular line and dust emission that is associated with strong water maser emission (W3(H2O)). Figure 10 shows the footprint of one of the subarrays in the [CII] line towards the source central position. [CII] absorption by gas on the line-of-sight is recorded for the central pixel, towards the continuum of the hot core. The continuum level towards the hot core can accurately be determined in these double-beam chopped observations. As explained in Sect. 3.3.3, total power observations would not allow deriving a reliable continuum level.

4.2. Horsehead large mapping demonstration

After the successful technical commissioning of the LFA, the SOFIA Director granted discretionary time for a high-visibility science project to demonstrate the new opportunities for velocity-resolved spectroscopy to the SOFIA user communities. On SOFIA flight 267 on December 11, 2015, the [CII] emission from a large field towards the Horsehead nebula was recorded during an allocated time slot of four hours. The field, 17.5′ × 12.5′ in size, was fully sampled (6″step size) in

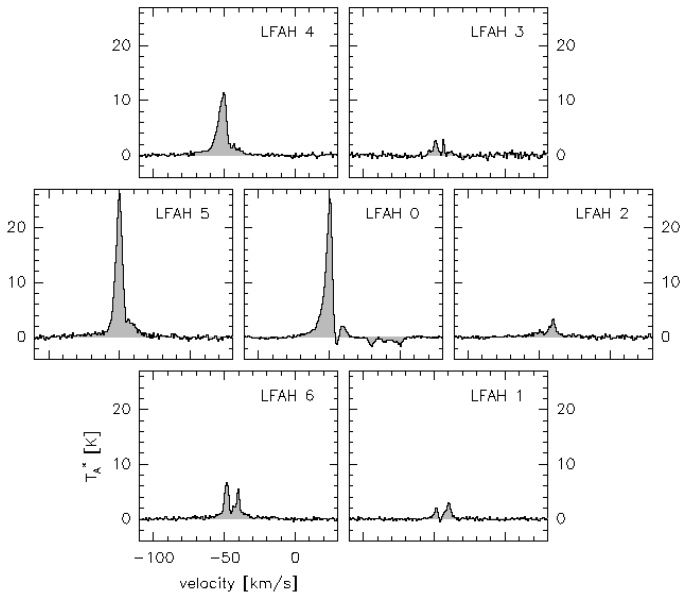

Fig. 10. Spectra for one of the upGREAT sub-arrays taken around the central position of the compact HII region W3(OH) (a polynomial baseline of order 0 was subtracted). In the central pixel, towards the continuum of the hot core, [CII] absorption by gas on the line-of-sight is recorded.

total power on-the-fly observing mode. The field was substructured into four subfields, with redundant mapping (each subfield was covered four times with alternating scanning directions and rotated array geometry). Figure 11 shows two maps showing the distribution of CII emission, integrated over the velocity ranges 9.5 to 11.5 km s^{-1}and 13 to 15 km s^{-1}. The sensitivity across the map is extremely uniform. The noise rms of the data cube, for a spectral resolution of 0.19 km s^{-1}, is 2 K in the velocity channels free of emission.

It is estimated that an equivalent map would have required over 50 h of observing time using *Herschel*/HIFI, which would amount to a gain of more than a factor of 10 in mapping speed using SOFIA.The data are publicly available to the astronomical community as a demonstration observation with upGREAT[3].

The line/continuum intensities in the repeated subfields are typically reproducible within ±5%. When roughly comparing the integrated fluxes over similar regions observed with *Herschel*/HIFI (around the Horsehead) and taking into account the respective beam couplings, we found the fluxes to agree within 15%, which is within HIFI and upGREAT calibration error bars.

5. Future work

We presented a novel multi-pixel spectrometer for observations at 1.9 THz, which was successfully commissioned onboard the SOFIA observatory in May and December 2015. First results of large scale mapping of various sources demonstrate the capabilities of this instrument. With upGREAT on SOFIA, it is now possible to efficiently map very large fields with very high spectral resolution within a few hours, with excellent receiver sensitivities, homogeneous noise performance across the map and stable spectral baselines. The next steps for this array will be to extend the usable RF bandwidth by utilizing a different local oscillator

[3] https://www.sofia.usra.edu/science/proposing-and-observing/proposal-calls/sofia-directors-discretionary-time/horsehead-nebula

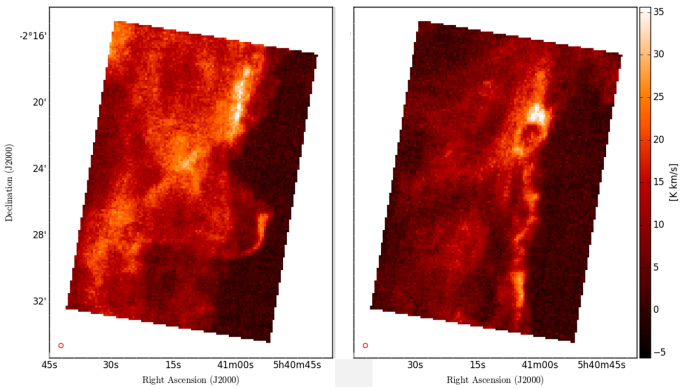

Fig. 11. Example of large scale mapping of the Horsehead nebula region, performed in four hours, covering a 17.5′ × 12.5′ field. The lower left red circle show the 15″ beam. We display two integrated channel maps at 9.5−11.3 km s^{-1} and 13−15 km s^{-1}, delineating the complex kinematics of the region. While strikingly prominent at optical wavelengths where it is seen as a dark patch, the Horsehead nebula [CII] emission is limited to the UV-illuminated edge of its PDR. The fine morphology of the IC 434 PDR interface displays beautifully.

technology with sufficient power. A second multi-pixel receiver to observe the [OI] atomic fine structure transition at 4.745 THz, the upGREAT HFA, is currently under integration and will be commissioned at the end of 2016. The two upGREAT arrays will be operated simultaneously.

Acknowledgements. The authors would like to thank the USRA and NASA staff of the Armstrong Flight Research Center in Palmdale and of the Ames Research Center in Mountain View as well as the DSI for their strong continuous support before and throughout the upGREAT LFA commissioning campaign. The development of upGREAT was financed by the participating institutes, by the Federal Ministry of Economics and Technology via the German Space Agency (DLR) under Grants 50 OK 1102, 50 OK 1103 and 50 OK 1104 and within the Collaborative Research Centre 956, sub-projects D2 and D3, funded by the Deutsche Forschungsgemeinschaft (DFG).

References

Adams, J. D., Herter, T. L., Gull, G. E., et al. 2010, in Ground-based and Airborne Instrumentation for Astronomy III, Proc. SPIE, 7735, 77351
Büchel, D., Pütz, P., Jacobs, K., et al. 2015, IEEE Trans. Terahertz Sci. Technol., 5, 207
Dunham, E. W., Elliot, J. L., Bida, T. A., et al. 2008, in Ground-based and Airborne Instrumentation for Astronomy II, Proc. SPIE, 7014, 70144
Graf, U. U. 2016, J. Infrared, Millimeter, and Terahertz Waves, 37, 770
Graf, U. U., Honingh, C. E., Jacobs, K., & Stutzki, J. 2015, J. Infrared, Millimeter and Terahertz Waves, 36, 896
Guan, X., Stutzki, J., Graf, U. U., et al. 2012, A&A, 542, L4
Heyminck, S., Graf, U. U., Güsten, R., et al. 2012, A&A, 542, L1
Klein, R., Poglitsch, A., Raab, W., et al. 2010, in Ground-based and Airborne Instrumentation for Astronomy III, Proc. SPIE, 7735, 77351
Klein, B., Hochgürtel, S., Krämer, I., et al. 2012, A&A, 542, L3
Pilbratt, G. L., Riedinger, J. R., Passvogel, T., et al. 2010, A&A, 518, L1
Pütz, P., Honingh, C. E., Jacobs, K., et al. 2012, A&A, 542, L2
Richter, M. J., Ennico, K. A., McKelvey, M. E., & Seifahrt, A. 2010, in Ground-based and Airborne Instrumentation for Astronomy III, Proc. SPIE, 7735, 77356
Risacher, C., Güsten, R., Stutzki, J., et al. 2016, IEEE Trans. Terahertz Sci. Technol., 6, 199
Shurakov, A., Lobanov, Y., & Goltsman, G. 2016, Superconductor Science Technology, 29, 023001
Smith, E. C., & McLean, I. S. 2008, in Ground-based and Airborne Instrumentation for Astronomy II, Proc. SPIE, 7014, 701411
Vaillancourt, J. E., Chuss, D. T., Crutcher, R. M., et al. 2007, in Infrared Spaceborne Remote Sensing and Instrumentation XV, Proc. SPIE, 6678, 66780
Young, E. T., Becklin, E. E., Marcum, P. M., et al. 2012, ApJ, 749, L17